APPLICATION OF FIBER OPTIC TEMPERATURE AND STRAIN SENSING TECHNOLOGY TO GAS HYDRATES

Shannon M. Ulrich
Biosciences Division, Oak Ridge National Laboratory
P.O. Box 2008, MS-6036, Oak Ridge, TN 37831-6036 USA

Megan E. Elwood Madden
School of Geology and Geophysics, University of Oklahoma
100 E. Boyd, Suite 810, Norman, OK 73019 USA

Claudia J. Rawn
Material Science and Technology Division, ORNL
P.O. Box 2008, MS-6064, Oak Ridge, TN 37831-6064 USA

Phillip Szymcek
Environmental Sciences Division, ORNL
P. O. Box 2008, MS-6036, Oak Ridge, TN 37831-6036 USA

Tommy Joe Phelps[*]
Biosciences Division, ORNL
P.O. Box 2008, MS-6036, Oak Ridge, TN 37831-6036 USA

ABSTRACT

Gas hydrates may have a significant influence on global carbon cycles due to their large carbon storage capacity in the form of greenhouse gases and their sensitivity to small perturbations in local conditions. Characterizing existing gas hydrate and the formation of new hydrate within sediment systems and their response to small changes in temperature and pressure is imperative to understanding how this dynamic system functions. Fiber optic sensing technology offers a way to measure precisely temperature and strain in harsh environments such as the seafloor. Recent large-scale experiments using Oak Ridge National Laboratory's Seafloor Process Simulator were designed to evaluate the potential of fiber optic sensors to study the formation and dissociation of gas hydrates in 4-D within natural sediments. Results indicate that the fiber optic sensors are so sensitive to experimental perturbations (e.g. refrigeration cycles) that small changes due to hydrate formation or dissociation can be overshadowed.

Keywords: gas hydrates, fiber optic sensors, natural sediments

INTRODUCTION

Natural gas hydrates occur widely throughout ocean sediments and in terrestrial soils in areas of permafrost. They are solid, crystalline structures of water molecules that contain cages large enough to hold various gas molecules. The most common gas hydrates found in nature are methane hydrate and carbon dioxide hydrate or a hydrate containing a mixture of the two gases. As a reservoir of greenhouse gases, natural gas and carbon, hydrates are of significant interest from both environmental and economic standpoints. Research indicates that

---
[*] Corresponding author: Phone: +1 865 574 7290 Fax +1 865 576 3989 Email: phelpstj@ornl.gov

hydrates are sensitive to changes in deep ocean conditions [1] and have the potential to influence global climate change by sequestering or releasing greenhouse gases [2]. Hydrates are also a potential source of natural gas for human energy consumption [3-4], though technologies have yet to be developed to make them an economic resource. While considerable research has been conducted to characterize hydrates in nature, gaps remain regarding geologic controls on hydrate formation, distribution and habit. Hydrates have been recovered in marine sediments across many active ocean margins, providing some information on these physical characteristics [5-11] (among others). All of this work shows us where we can find hydrate, but we know very little about how the hydrate formed.

Gas hydrate is most commonly recovered as disseminated particles in sediment. Because hydrate occurs on a small scale, a sensitive data-gathering system that collects data on a fine spatial scale is required. Recently, fiber optics-based sensing technology has been used in a variety of industrial applications including continuous measurement of temperature and strain down boreholes in order to better monitor conditions such as pressure in petroleum reservoirs and rock surrounding the borehole [12–14]. Fiber optic sensors are ideal in harsh environments that conventional pressure sensors cannot withstand [15]. Additionally, fiber optics can be manufactured with data-collection gratings at variable spacing, which makes them ideal to study changes in temperature and strain at a very fine scale. Fiber optics can measure temperature and strain with high precision via changes in conformation of the fiber, itself, in response to the expansion, contraction or bending conferred by environmental conditions. Because hydrate formation is exothermic and dissociation is endothermic, both can theoretically be recorded by fiber optics sensing technology in the form of temperature change over a finite period of time.

This work was designed to test the potential of fiber optics to monitor localized hydrate formation and dissociation in a simulated seafloor environment. The main objective was to use fiber optics to characterize where hydrate was most likely to form within natural sediments in four dimensions, as well as gaining insights with respect to rates of formation and dissociation and with respect to hydrate habits that are most likely to form in nature.

In order to test the application of fiber optic sensor technology within sediment-hydrate systems, the Biosciences Division of Oak Ridge National Laboratory has conducted a series of experiments to calibrate and test the response of sensors to temperature and pressure changes, as well as hydrate formation and dissociation. We conducted an ex-situ fiber test which took place outside of our experiment vessel and was designed to provide an absolute temperature reference to calibrate our data. Four control homogenous sediment experiments using nitrogen gas were conducted to monitor fiber response to pressure and temperature changes in a hydrate-free system. Three homogenous sediment experiments were conducted using hydrate-forming methane gas to measure the response of the fibers to hydrate formation and dissociation (Table 1). The homogenous sediment experiments contained sieved quartz sand. The goal of these week-long sediment experiments has been to evaluate the usefulness of fiber optics technology to map where and how hydrates are likely to form in natural sediments.

Experiment type	No. of fibers	Dissociation method	Days
ex-situ fiber test	4	N/A	2
nitrogen	4	warm	3
nitrogen	4	warm	3
nitrogen	4	depressurize	2
nitrogen	4	depressurize	3
methane	3	depressurize	7
methane	3	warm	7
methane	4	warm	7

Table 1. Experiments to date.

MATERIALS AND METHODS
Distributed Sensing System
Data was collected using a fiber optics-based Luna® Distributed Sensing System (DSS) that records small changes in temperature and strain every one centimeter over the length of a thin optical fiber (Figure 1). Readings were taken every 15 seconds for the 5-2007 methane experiment and every minute for other experiments.

Due to the particular fiber optic technology the DSS utilizes, it cannot differentiate between changes in temperature and strain; therefore, data is recorded as a temperature and strain hybrid, referred to here as the Temperature Strain Value (TSV).
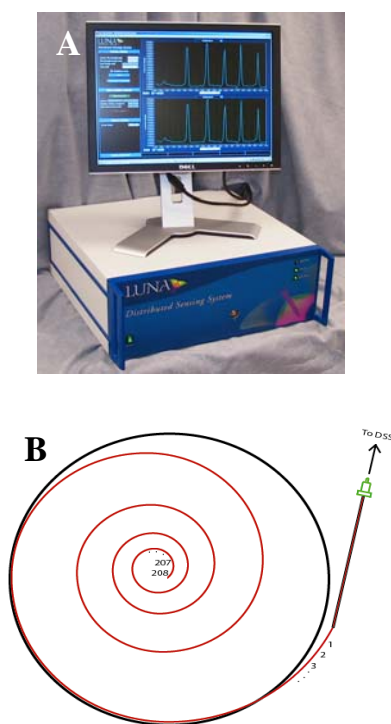
Figure 1. The Luna® Distributed Sensing System (A) uses laser pulses to determine changes in shape of the optical fiber due to temperature and strain changes at 1-cm intervals along the length of the fiber (B), diagrammed here in red in a spiral conformation. The laser light is reflected at each 1-cm sensor grating. Temperature and strain cause the fiber to expand, contract, and/or bend, all factors which are notable in the reflection time. The time it takes for the reflection to return to the DSS is translated into a hybrid temperature strain value (TSV).

The system and accompanying software are designed to take baseline information of the fibers and eliminate background effects or other influences relating to the individualities of a given fiber. The data gathered should show only changes in TSV local to the fiber.

Each fiber was coiled in a spiral and attached to a circle of plastic mesh, with the beginning of the fiber on the outside of the spiral and the end of the fiber at the center of the spiral; thus, the further the distance along the fiber, the closer to the center of the spiral. This setup created a two dimensional "fiber plane" over which the fiber could record TSV.

Ex-situ fiber test
In order to calibrate the DSS data with actual temperature data, a simple experiment was conducted in which data was simultaneously gathered by DSS fibers and a thermocouple accurate to 0.5º C. The fibers and the thermocouple were exposed to the same environmental conditions.

The thermocouple and four DSS fiber planes were stacked in the bottom of a 10 gallon plastic bin containing 10 cm of room-temperature water (18.9º C). The fiber planes were weighted with another circle of plastic mesh and a large, round brass sieve to prevent floating. The fibers were zeroed under these conditions and collected baseline data for 70 minutes, at which point the bin was filled to 40 cm with ice water. After the addition of the ice water, the temperature recorded by the thermocouple was 1.32º C. Data collection continued overnight until the ice melted and the system again reached baseline conditions.

Nitrogen control experiments
In order to assay the performance of fibers and sensors in an experimental setting without the added complexity of changing temperatures and strain due to hydrate formation and dissociation, we conducted four homogenous sediment experiments only using nitrogen gas, which does not form gas hydrate within the temperature-pressure field of these experiments.

Experiments were conducted in a 33-L PVC bucket with polycarbonate windows. 14 liters of 30% water-saturated, sieved (<500 micron grain size) commercially available Ottawa sand was placed inside the bucket, layered with three or four data-gathering fiber optics planes. Two thermocouples recorded temperature in the

headspace and/or were submerged in the top 20 cm of sediment. The bucket was placed inside Oak Ridge National Laboratory's Seafloor Process Simulator, a cylindrical 72-L volume Hastelloy C-22 vessel with 42 sampling ports, including 2 sapphire windows, capable of maintaining
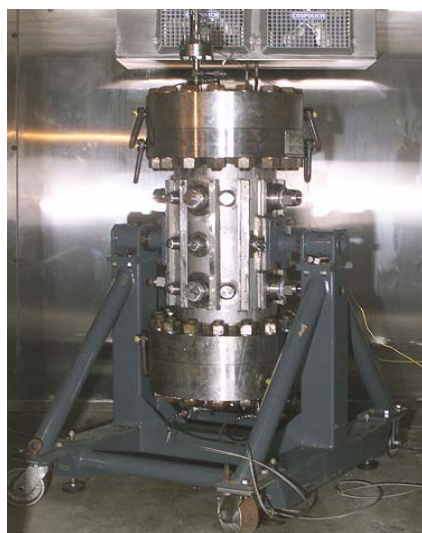

Figure 2. ORNL's Seafloor Process Simulator (SPS), a 72-L Hastelloy vessel capable of withstanding pressures and temperatures comparable to those encountered within the hydrate stability zone.
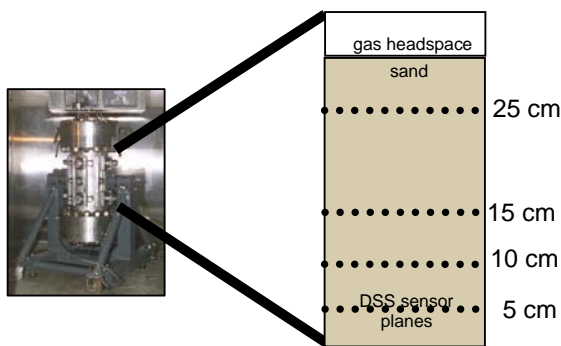

Figure 3. This diagram shows the setup of the sediment system inside the SPS. The bucket is filled with 30% water-saturated sand, layered with three or four DSS sensor planes at 5, 10 (when a fourth fiber is used), 15 and 25 cm from the bottom of the bucket.

pressures up to 20 MPa *[16]*, see Figure 2. The SPS was housed in an explosion-proof coldroom and cooled to ~1 °C for the duration of each experiment. The optical fibers were connected to the DSS through a pass-through port in the side of the SPS. Optical fibers used ranged in length from 100 to 400 centimeters (100 to 400 sensors).

The system was set up the day before the experiment: all experiments were set up using chilled sand mixed with chilled water to 30% water saturation and layered with fiber planes within the bucket, except the 5-2007 methane experiment, which used room temperature sand and water (Figure 3). The bucket was placed within the SPS, the optical fibers were connected, and the SPS was sealed and placed within the coldroom. The system was pressurized with nitrogen to ~600 psi (4.1 MPa), well outside the 3-phase stability field as calculated using the CSMHYD hydrate stability model *[17]*. To simulate an experiment using a hydrate-forming gas, we left the system at pressure overnight to saturate the water with gas.

After 20 hours, we boosted the pressure to ~1300 psi (9 MPa-well within the hydrate stability field had methane been used as the pressure medium) and began logging both DSS and LabView data. After 2 days in the nitrogen experiments and 5 days in all others, the SPS was either depressurized, then warmed or warmed, then depressurized to simulate hydrate dissociation triggers.

Of the four nitrogen experiments, two ended in depressurization and then turning off the coldroom, and two ended by turning off the coldroom and then depressurizing. For the second trial of each experiment type, the fibers were redistributed in the sediment. Changing the order of the fibers allowed us to deduce whether the unique signature of a particular fiber was due to its location or due to artifacts resulting from the individualities of the fiber, itself.

Methane experiments
All materials and methods of these experiments were the same as the homogenous sediment experiments using nitrogen except that methane was used instead of nitrogen and the vessel was flushed with nitrogen before and after running the each experiment for safety reasons. The methane experiments also lasted longer than the nitrogen experiments to allow time for hydrate formation and dissociation.

RESULTS AND DISCUSSION
Ex-situ fiber test
Figure 4 shows the top view of 4 plots, each representing data gathered by one spiraled fiber. The x-axis is the duration of the experiment in minutes, the y-axis is the TSV, and the z-axis is distance along the fiber in centimeters. Because the fiber is coiled in a spiral, the system is easiest to visualize by noting that the further you are along the fiber, the closer you are to the center of the spiral.

All fibers precisely record the addition of ice water to the room temperature water already in the bucket at minute 70. Each fiber also records an abrupt and uniform temperature increase beginning in the center of each fiber spiral and moving out toward the edge of the spiral over time, creating the conspicuous curve visible on each plot. This temperature increase is due to the melting of the ice in the bucket. The delay in warming from the center of the spiral out can be attributed to restricted warm water advection near the edge of each fiber spiral due to the presence of the round sieve sitting on top of the fiber stack. Even the slow rate of temperature communication in advecting water creates a distinct signature on the data, showing the fibers' sensitivity.

None of the fibers recorded accurate absolute temperatures though a roughly consistent offset of ~ -25° C from the absolute temperature was recorded consistently by certain sensors on each fiber. More work needs to be done to determine if the offset is systematic enough for us to deduce absolute temperatures from current data.

Nitrogen control experiments
Figure 5 shows data from two nitrogen control experiments. We used identical methods in each experiment except that the fibers were redistributed between experiments. Each plot in Figure 5 represents one spiral plane within the sediment of our cylindrical experiment vessel. The location of each fiber plane is indicated in cm from the bottom of the experimental vessel.

DSS data logging was initialized after boosting the pressure of the system to 1200-1300 psi (8.3-9 MPa). Data from all fibers show the major events of the experiment: initial cooling of the coldroom (denoted along the x-axis as a green square), equilibrium (yellow star), and finally depressurization or warming of the system, depending on the technique used, to force

"dissociation". Depressurization can be seen in the data as a steep ridge or spike at a distinct time and is denoted by a blue triangle.

All fibers from both experiments show similar overall trends (except for fiber 115 which will be discussed later): at the beginning, the TSV is roughly the same across the length of each entire fiber and no sensors report any local TSV changes before depressurization at 150 minutes. Depressurization drives a steep decrease in TSV which is more intense near the beginning of each fiber. Although these trends are notable in all fibers, fiber 115 appears to be more sensitive than the other fibers, reporting undulating TSVs along its length. It should be noted that fiber 115 is older than any of the other fibers used in these experiments and might record TSVs differently because it was manufactured at a different time. Results indicate that fiber 115 gathers data that is incongruous to that of the other fibers regardless of location.

Even in the absence of hydrate formation or dissociation, some ridges and peaks are visible in the nitrogen experiment data. The ridges occur most conspicuously on the 5 cm and 15 cm planes and occur over half or the entire length of a fiber. These ridges are artifacts of these particular fibers. A number of small troughs just after depressurizing are visible in most of the plots. These are of insignificant duration (<10 minutes) when compared to the methane experiments which lasted >7000 minutes; thus the small troughs can be ignored.

Methane experiments
Figure 6 shows data from two homogenous sediment methane experiments where each plot represents data from one fiber plane within the sediment.

Dissociation driven by depressurizing:
The fibers in the 5-2007 experiment report trenches constrained to only the first 50 centimeters of the two uppermost fiber planes. These trenches occur after depressurizing at 5200 minutes and might represent hydrate dissociation as indicated by local cooling around the outermost part of the sediment column. Areas of proposed hydrate formation and dissociation are denoted in Figure 6 by upward and downward arrows, respectively. The edge of the sediment column is the most likely place for hydrate formation and
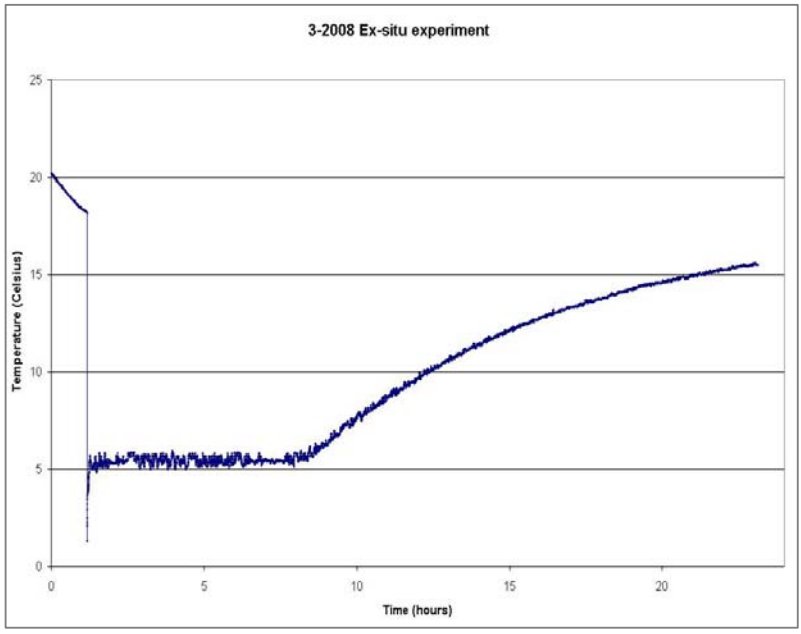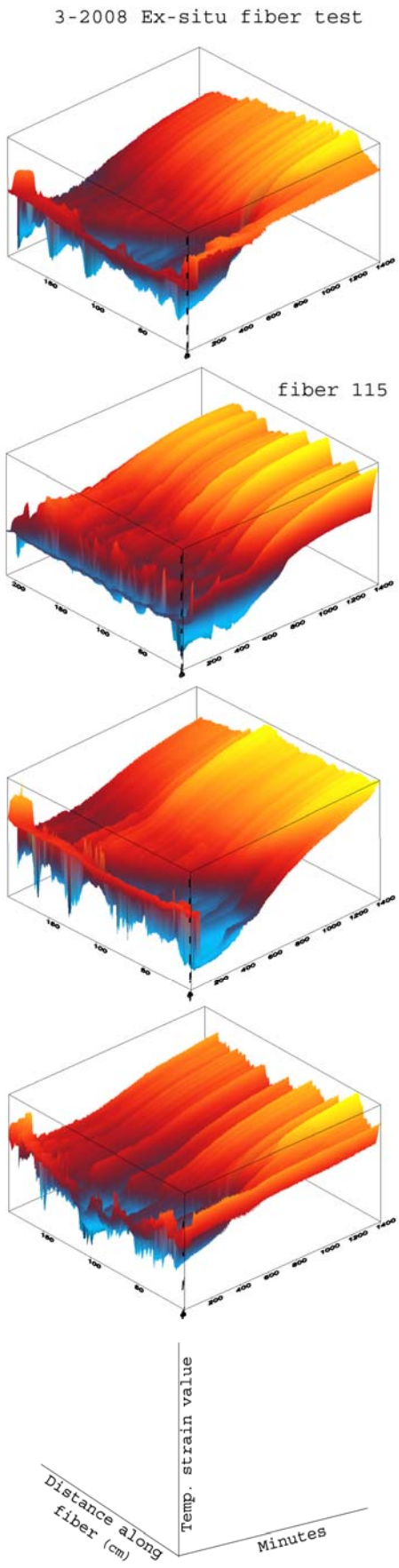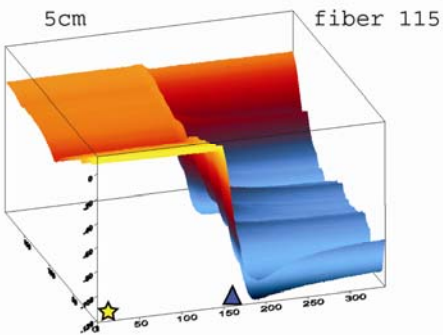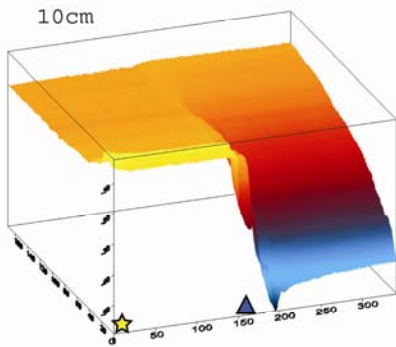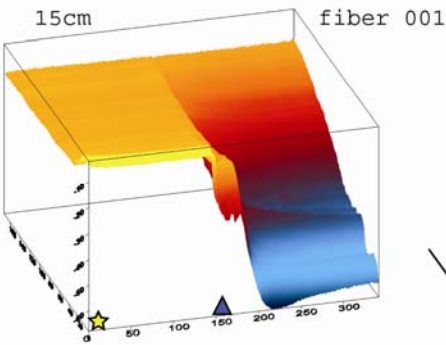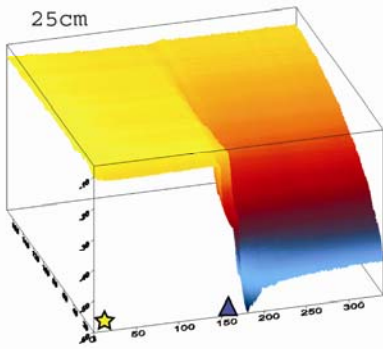
Figure 4. DSS data from the 3-2008 Ex-situ fiber test via the DSS (left) and thermocouple data (top). Axes in the DSS data plots are as follows: x-axis is time in minutes, y-axis is TSV (zero is in the center of the axis) and z-axis is the distance along the optical fiber in centimeters starting from the origin. Yellow indicates the warmest temperatures while light blue indicates the coldest.

The fibers record temperatures offset by roughly -25º C from the absolute temperature recorded by the thermocouple. The addition of ice water to the room temperature water is visible at minute 70 as a steep fall in temperatures across the entire length of each fiber and in the thermocouple plot above. Temperatures gradually rise, starting from the inside of each fiber spiral. This conspicuous warming pattern is likely due to restricted warm water advection around the edges of the fiber spirals due to the sieve sitting on top of them.

2-2008 30% H2O saturated homogenous
sediment NITROGEN experiment;
dissociation by depressurizing

25cm

15cm   fiber 001

10cm

5cm   fiber 115

2-2008 30% H2O saturated homogenous
sediment NITROGEN experiment;
dissociation by depressurizing

25cm
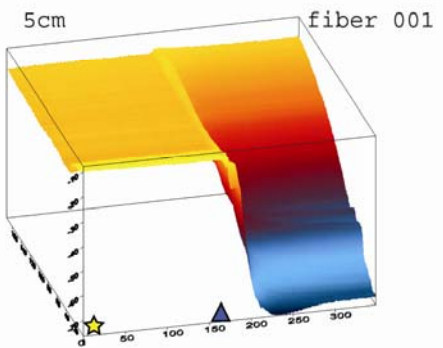
Fiber not functional.

15cm   fiber 115

10cm

5cm   fiber 001

Temp. strain value
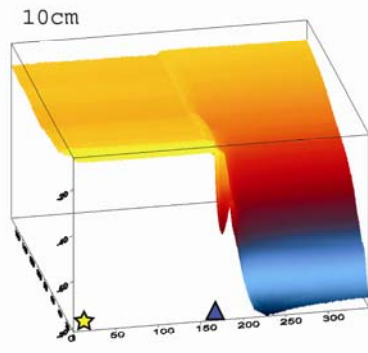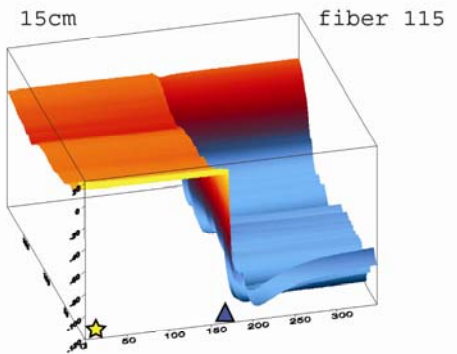
Distance along fiber (cm)

Minutes

Figure 5. Data from two nitrogen control experiments, both featuring depressurization around minute 160 (blue triangle). The yellow star indicates when the system reached equilibrium. The fibers were redistributed between trials to establish which data trends were due to location within the bucket and which were fiber artifacts.
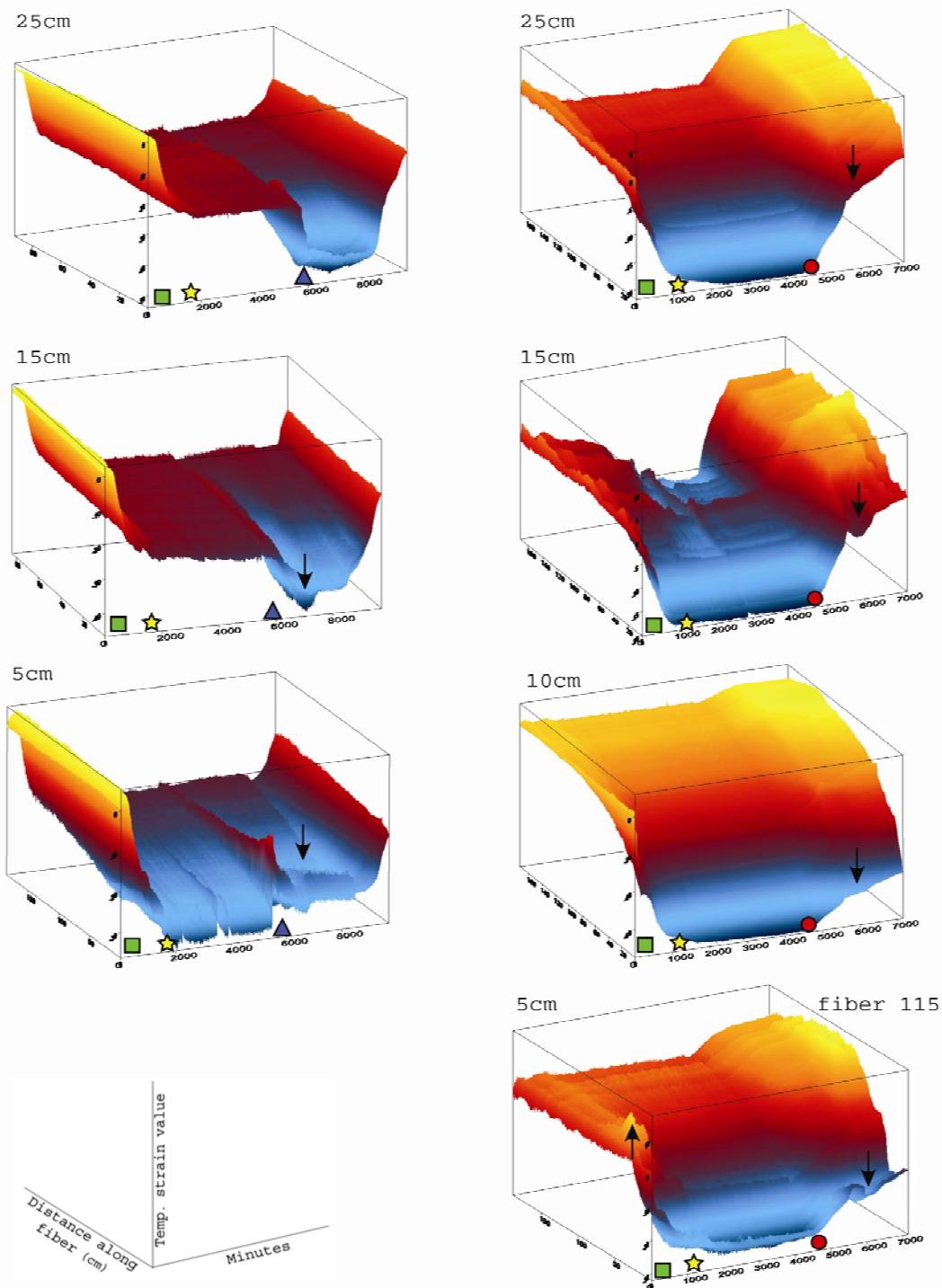
Figure 6. Data from the 5-2007 and 1-2008 methane experiments. The green square denotes the initial cooling of the systems and the yellow star marks when the systems reached equilibrium. Dissociation was forced by depressurizing in the 5-2007 experiment (blue triangle) and by warming in the 1-2008 experiment (red circle). Upward-pointing arrows indicate peaks in hydrate formation and downward-pointing arrows indicate troughs representing dissociation.

dissociation, for two reasons: 1) it is likely colder/warmer due to air circulation between the outside of the experimental vessel and the inside of the SPS, and 2) there is likely a higher concentration of methane due to vertical conduits in the sediment created by inserted thermocouples, fibers and the vertical windows of the experimental vessel, itself.

Dissociation driven by warming:
Data from all fibers showed initial cooling across the complete length of the fibers, displayed as a decrease in the TSV for the first 200 minutes. Peaks representing hydrate formation can be seen in the 1-2008 methane experiment in the 5 cm and 15 cm fiber planes between 200 and 800 minutes. Beyond 800 minutes, the TSV follows a similar sloping trend throughout all four fibers that shows decreasing TSV toward the beginning of each fiber (the edge of the vessel). The coldroom was turned off just before 5000 minutes as denoted by a red circle and all fibers recorded gradual warming thereafter. Warming can be seen as a change in trend of the TSV (an inflection point) at a distinct time and can be seen particularly well along the bottom of any of the 1-2008 plots as a general upward trend of the TSV. Troughs representing hydrate dissociation can be seen in the 5 cm and 15 cm fiber planes just before 6000 minutes. TSV flatlines possibly representing a small amount of hydrate dissociation can be seen in the 10 cm and 25 cm fiber planes. This type of flatline has been seen before in our large scale hydrate experiments where the dissociation causes just enough cooling to cancel out the rate of warming after the coldroom is turned off *[18]*.

CONCLUSIONS AND FUTURE WORK
Data from the fibers conclusively indicates that the DSS fibers do not accurately communicate absolute temperature or temperature changes even when strain is held constant as in the ex-situ experiment.

The initial hope was that the optical fibers would record only changes in temperature and strain immediately local to the fiber. Our results indicate that the imprint of larger environmental changes, such as the warming, cooling or vibrations of our coldroom, may in some cases overshadow the fine-scale changes in temperature and strain due to hydrate formation and dissociation in our system. Trends that span the entire length of a fiber at one point in time are due to major environmental events which occur at that point in time (e.g. changes in coldroom temperature or vessel pressure.) Trends that span the entire length of the experiment at a single location on the fiber can be considered artifacts of the fiber. That said, it is still possible to see some indications of hydrate formation and dissociation when looking at the data in small sections. For example, in the 5-2007 methane experiment, prominent recurring troughs dominate sensors 1-40 after depressurization. Each trough represents a finite change in TSV over a finite period of time, after which the TSV returns to some level of stasis before entering the next irregular trough. Data such as this indicates that fiber optics might be a useful tool in monitoring hydrate formation and dissociation under extremely controlled conditions where temperature and strain changes local to the fiber are the dominant signature in the data.

Our results also suggest that the great sensitivity of these optical fibers might make them unsuitable for other applications such as monitoring the conditions of rock surrounding a borehole. These fibers are so sensitive to changes in local conditions that the data recorded most likely represents changes near the fiber, rather than changes in the conditions several cm distant.

The sensitivity of these fibers demands that we refine our experimental methods such that changes in temperature and strain not due to hydrate formation or dissociation are minimized.

We are also currently working on a way to plot the TSV using polar coordinates; for example, by measuring the location of each sensor on a fiber plane and assigning the TSV to that location, we can plot the TSV in a spiral as it actually occurs in the vessel at a given time. Such a three dimensional representation would provide a much better idea of the spatial distribution of hydrate formation and dissociation.

REFERENCES

[1] Buffett B, Archer D. *Global inventory of methane clathrate: sensitivity to changes in the deep ocean.* Earth and Planetary Science Letters 2004; 227(3-4): 185-199.

[2] Dickens GR. *Methane hydrates in quaternary climate change – The clathrate gun hypothesis.* Science 2003; 299(5609):1017-1017.

[3] Milkov AV, Sassen R. *Economic geology of offshore gas hydrate accumulations and provinces.* Journal of Marine and Petroleum Geology 2003; 19:1-11.

[4] Moridis GJ and Sloan ED. *Gas production potential of disperse low-saturation hydrate accumulations in oceanic sediments.* Energy Conservation and Management 2007; 48(6):1834-1849.

[5] Brooks JM, Field ME, Kennicutt MC, II. *Observations of gas hydrates in marine sediments, offshore northern California.* Marine Geology 1991; 96:103-109.

[6] Charlou JL, Donval JP, Fouquet Y, Ondreas H, Knoery J, Cochonat P, Levache D, Poirier Y, Jean-Baptiste P, Fourre E, Chazallon B. *Physical and chemical characterization of gas hydrates and associated methane plumes in the Congo-Angola Basin.* Chemical Geology 2004; 205:405-425.

[7] Ginsburg GD, Soloviev VA, Cranston RE, Lorenson TD, Kvenvolden KA. *Gas hydrates from the continental slope, offshore Sakhalin Island, Okhotsk Sea.* Geo-Marine Letters 1993; 13:41-48.

[8] Ginsburg G, Soloviev V, Matveeva T, Andreeva I. *Sediment grain-size control on gas hydrates presence, sites 994, 995, and 997*, in Paull CK, Wallace PJ, Dillon, editors: Proceedings of the Ocean Drilling Program, Scientific Results. 164:237-245.

[9] Kvenvolden KA, MacDonald TJ. *Gas hydrates of the Middle America Trench-Deep Sea Drilling Project Leg 84*, in von Huene R, Aubouin J and others: Initial Reports of the Deep Sea Drilling Project. U.S. Government Printing Office: Washington DC, 1985; 84:667-682.

[10] Matveeva TV, Mazurenko LL, Soloviev VA, Klerkx J, Kaulio VV, Prasolov EM. *Gas hydrate accumulation in the subsurface sediments of Lake Baikal (Eastern Siberia).* Geo-Marine Letters 2003; 23:289-299.

[11] Sassen R, Losh SL, Cathles L, III, Roberts HH, Whelan JK, Milkov AV, Sweet ST, DeFreitas DA. *Massive vein-filling gas hydrate: relation to ongoing gas migration from the deep subsurface in the Gulf of Mexico.* Journal of Marine and Petroleum Geology 2001; 18:551-560.

[12] Schroeder RJ, Romos RT, Yamate T. *Fiber optic sensors for oilfield services*. Proceedings of SPIE 1999; 3860:12-22.

[13] Mendez A, Dalziel R, Douglas N. *Applications of optical fiber sensors in subsea and downhole oil well environment.* Proceedings of SPIE 1999; 3860:23-34.

[14] Flecker MJ, Thompson SJ, McKay CS, Buchwalter JL. *Maximizing production with permanent downhole sensors.* Journal of Petroleum Technology 2000; 52(10):62.

[15] Xiao H, Deng JD, Wang ZY, Huo W, Zhang P, Luo M, Pickrell GR, May RG, Wang A. *Fiber optic pressure sensor with self-compensation capability for harsh environment applications.* Optical Engineering 2005; 44(5): article 054403.

[16] Phelps TJ, Peter DJ, Marshall SL, West OR, Liang L, Blencoe JG, Alexiades V, Jacobs GK, Naney MT, Heck Jr JL. *A new experimental facility for investigating the formation and properties of gas hydrates under simulated seafloor conditions.* Review of Scientific Instruments 2001; 72(2):1514-1521.

[17] Sloan ED. *Clathrate Hydrates of Natural Gases, 2nd edition.* New York: Marcel Dekker, 1998.

[18] Riestenberg D, West O, Lee S, McCallum S, Phelps TJ. *Sediment surface effects on methane hydrate formation and dissociation.* Marine Geology 2003; 198:181-190.